Title: Mechanistic home range capture-recapture models for the estimation of population density and landscape connectivity

Keita Fukasawa

Biodiversity Division, National Institute for Environmental Studies
16-2 Onogawa, Tsukuba, Ibaraki, 305-8506 Japan
k.fukasawa37@gmail.com

Running head: Advection-diffusion capture-recapture models

Abstract

Spatially explicit capture-recapture (SECR) models provide an integrative statistical tool for analysing animal movement and population patterns. Although incorporating home range formation with step selection functions into SECR can improve the prediction of animal space use in a heterogeneous landscape, this approach is challenging owing to the sparseness of recapture events.

In this study, I developed an advection-diffusion capture-recapture model (ADCR), which is an extension of SECR incorporating home range formation with advection-diffusion formalism, providing a new framework to estimate population density and landscape connectivity. I tested the unbiasedness of the estimator and robustness to the landscape resolution using simulated capture-recapture data generated by a step selection function. I also compared parameter estimates with those from a spatial capture-recapture model based on the least cost path (SCR-LCP) and basic SECR.

Population density, connectivity, and home range estimates of ADCR were unbiased over randomly determined sets of true parameters. Although the accuracy of density estimates by ADCR was nearly identical to those of existing models, home range shape could be predicted more accurately by ADCR than by SCR-LCP. ADCR was robust to the choice of landscape resolution, which is a favourable characteristic in random walk-based connectivity measures.

ADCR provides unique opportunities to elucidate both individual- and population-level ecological processes from capture-recapture data. By offering a formal link with step selection functions to estimate animal movement, it is suitable for simultaneously modeling with capture-recapture data and animal movement data. This study provides a basis for studies of the interplay between animal movement processes and population patterns.

Key words: spatial capture-recapture, circuit theory, landscape resistance, abundance estimation, mechanistic home range analysis, partial differential equation, step selection function,

advection-diffusion equation

Introduction

Anthropogenic activity leads to habitat loss and fragmentation, posing a major threat to biodiversity. In a fragmented landscape, connectivity between habitat patches affects population patterns and sustainability (Hanski et al., 1994). Functional connectivity in a heterogeneous landscape is not only of general interest in basic ecology but also a key factor affecting decision-making in wildlife management and conservation (Goodwin & Fahrig, 2002; Royle et al., 2018; Osada et al., 2019). Circuit theory and least cost path (LCP) modeling are two major paradigms for evaluating landscape connectivity, with different underlying behavioural assumptions and statistical properties (McRae et al., 2008; Marrotte & Bowman, 2017). Connectivity based on circuit theory has explicit links with animal movement models, such as random walks and step selection functions (McRae, 2006; Duchesne et al., 2015), and models of animal gene flow and movement have numerous applications (Dickson et al., 2019). Empirical determination of connectivity parameters, such as conductance of land cover types, is important to improve objectivity, and the development of estimators is a major challenge in ecology (Ovaskainen, 2004; Ovaskainen et al., 2008; Beyer et al., 2016; Signer et al., 2017; Osada et al., 2019).

Spatially explicit capture-recapture models (SECRs) are powerful tools with the capacity to estimate individual movement processes and population abundance in an integrative manner (McClintock et al., 2022). Although random-walk-based connectivity measures have favourable properties for practical applications, such as robustness to the resolution of landscape data (Marrotte & Bowman, 2017) and a straightforward link with movement models (Diniz et al., 2020), they are not as well-studied as LCP-based estimators (Royle et al., 2013; Sutherland et al., 2015; Fuller et al., 2016). In particular, the process of home range formation considering random-walk-based connectivity and site fidelity has been studied extensively by step selection

functions in movement ecology (Thurfjell et al., 2014; Duchesne et al., 2015; Signer et al., 2017; Péron, 2019; Potts & Schlägel, 2020). The corresponding SECR estimator can provide insight into the relationship between individual-level displacement and population-level abundance patterns. However, the temporal sparseness of capture-recapture data limits the application of SECR to complex movement processes (McClintock et al., 2022).

Incorporating mechanistic models of home range formation into SECR can enable inferences about connectivity as well as population abundance from capture-recapture data in a computationally tractable manner. Mechanistic home range analysis (Moorcroft & Lewis, 2006; Moorcroft & Barnett, 2008) is an analytical approach that ties the process of animal movements to the resultant home range shape. The approach has contributed to the development of advection-diffusion equations (ADE) to obtain flexible home ranges and likelihood-based modeling to estimate parameters empirically. ADEs describe deterministic drift to a focal point (e.g., an activity center) as advection terms and random walks as diffusion terms. Circuit theory is analogous to a diffusion process with heterogeneous diffusivity (Hanks & Hooten, 2013), and ADEs with heterogeneous diffusion coefficients in space are applicable to home ranges formed by animal movement affected by landscape resistance. Although a closed-form analytical solutions of ADEs rarely exist, computationally efficient ways to obtain a numerical solution have been developed (Hirsch, 2007). By integrating mechanistic home range analysis into SECR, the simultaneous estimation of connectivity and population density is possible, without substantial computational costs. Hereafter, I refer to this new SECR approach as the advection-diffusion capture-recapture model (ADCR).

Although ADCRs and LCP-based spatial capture-recapture models differ with respect to connectivity assumptions (LCP-SCR, Royle et al., 2013; Sutherland et al., 2015; Royle et al., 2018) and cannot be directly compared, evaluations of the performance of estimators are helpful for users. Applying statistical models to simulated data generated from a mechanistic animal movement model is a straightforward way to test the unbiasedness of estimators and robustness

to deviation from assumptions (Dupont et al., 2022; Theng et al., 2022). In particular, deviations in the spatial resolution of landscapes can often alter the results of landscape ecology (Qi & Wu, 1996; Turner et al., 1989), and the robustness of models to differences in spatial resolution between data generation and model estimation should be evaluated.

The aim of this study was to develop a formal framework for ADCR and to compare the accuracy of the estimated abundance and home range shape with those obtained by LCP-SCR under a random walk-based movement process. The identification of the optimal model is outside of the scope of this paper. Rather, my aim is to establish the merit of the ADCR under animal movement modeled by a step selection function, which is common in movement ecology. I specifically focused on a common situation in which the resolution of landscape factors is lower than that of the data generating process, and I tested the robustness of connectivity estimates to a decreased resolution. I also compared density estimates with those of basic SECR (Borchers & Efford, 2008) as a null model of heterogeneous connectivity. I predict that all three methods, ADCR, LCP-SCR, and basic SECR, will accurately estimate population densities because SECR is robust to the violation of home range assumptions (Efford 2019). I also predict that ADCR will have an advantage in estimating the effect of landscape on connectivity, as it is robust to the resolution of input data.

Material and Methods

Model Framework

ADCR is an extension of SECR in which animal home ranges were modeled as equilibrium solutions of the advection-diffusion equation, an Eulerian representation of the 2D Ornstein-Uhlenbeck (OU) process of animal movement in a heterogeneous connectivity landscape. By integrating the advection-diffusion equation with SECR, it is possible to

simultaneously estimate population density while inferring the effect of landscape connectivity on the skewed shape of the home range using capture-recapture data. Here, I describe the model structure of ADCR.

The OU process (Smouse et al., 2010) is a biased random walk with limit $\Delta t \rightarrow 0$ and is formalised by a stochastic differential equation for constant drift toward an activity center, $\boldsymbol{\mu} = (\mu_x, \mu_y)$, and a Brownian motion term. In this study, we consider the situation that the diffusion coefficient varys in space as follows:

$$d\mathbf{s}_t = c(\boldsymbol{\mu} - \mathbf{s}_t)dt + \sigma(\mathbf{s}_t)d\mathbf{W}_t \qquad \text{(eqn. 1)}$$

where $\mathbf{s}_t = (x_t, y_t)$ is the animal location at time t, $\mathbf{W}_t$ is the 2D independent Wiener process, c is the intensity of drift, and $\sigma(\mathbf{s}_t)$ is the standard deviation of the Wiener process, corresponding to the step length per unit time depending on the location. For the special case when $\sigma(\mathbf{s}_t)$ is constant over space, the probability distribution of $\mathbf{s}_t$ conditional on the initial location $\mathbf{s}_0$ is a bivariate normal distribution as follows (Dunn & Gipson, 1977):

$$p(\mathbf{s}_t|\mathbf{s}_0) = N\left(\exp(-ct)\mathbf{s}_0 + \left(1 - \exp(-ct)\right)\boldsymbol{\mu}, \frac{\sigma^2}{2c}\left(1 - exp(-2ct)\right)\mathbf{I}\right). \qquad \text{(eqn. 2)}$$

For the limiting case of $t \rightarrow +\infty$, this distribution converges to a static bivariate normal distribution, a default home range assumption for basic SECRs (Borchers & Efford, 2008; Royle et al., 2009).

In contrast to the above Lagrangian approach describing the microscopic displacement of an individual, the Eulerian approach treats movement as the macroscopic flow of the probability density of individual locations. It is described by the Fokker-Planck equation, a partial differential equation that describes the time evolution of the probability density in space (Moorcroft & Lewis, 2006). Let p denote the probability density of individual location; the corresponding Fokker-Planck equation for eqn. 1 is as follows:

$$\frac{\partial p}{\partial t} = -c\left((\mu_x - x)\frac{\partial p}{\partial x} + (\mu_y - y)\frac{\partial p}{\partial y}\right) + D(x, y)\left(\frac{\partial^2 p}{\partial x^2} + \frac{\partial^2 p}{\partial y^2}\right) \qquad \text{(eqn. 3)}$$

where $D(x, y) > 0$ is the diffusion coefficient. The first term on the right-hand side is advection corresponding to drift toward the activity center, and the second term is random diffusion. The

diffusion coefficient is interpreted as conductance in terms of circuit theory (McRae, 2006; McRae et al., 2008). To model the effect of environmental factors on connectivity, I applied the log-linear model $\ln(D(x, y)) = \beta_0 + \boldsymbol{\beta}\mathbf{z}(x, y)$, where β_0 is the intercept, $\mathbf{z}(x, y)$ is a vector of environmental variables at location (x, y), and $\boldsymbol{\beta}$ is the corresponding regression coefficients determining the contributions of environmental factors to landscape connectivity. For the special case when σ is constant over space, $D(x, y) = \sigma^2/2$. The intensity of drift, c, takes a positive value, and $\ln(c)$ is denoted by parameter α_0. To ensure that the volume of p is constant over time, the reflecting boundary condition is given for space.

Similar to mechanistic home range analysis (Moorcroft & Lewis, 2006), home range in this system is defined as the equilibrium probability density distribution, $p^*(\mathrm{x}, \mathrm{y}; \boldsymbol{\mu})$, which is the solution of p when $\delta p/\delta t = 0$ subject to the condition that $\int_{\mathcal{S}} p \, d\mathbf{s} = 1$, where $\mathcal{S}$ is the spatial domain. Note that α_0 and β_0 are redundant at the equilibrium state because $\ln(D(x, y)/c) = \beta_0 - \alpha_0 + \boldsymbol{\beta}\mathbf{z}(x, y)$. To ensure the identifiability of the model, it was reparametrized by $\gamma_0 = \beta_0 - \alpha_0$. γ_0 is interpreted as the logarithm of the relative intensity of diffusion and drift, which determines the average home range size. Although the closed-form solution rarely exists when $D(x, y)$ varies in space, it can be numerically solved by a variety of discretization techniques, such as the finite difference method and finite element method (Hirsch, 2007). In this study, the finite difference method was applied because it is suitable for common situations in which landscape factors affecting the diffusion coefficient are available as a raster dataset. In this study, grid cells of raster data were used to discretize space for simplicity. Technical details for discretization and numerical derivation of p^* are shown in Appendix S1.

To estimate connectivity parameters and population density simultaneously from capture-recapture data, the numerical solution of p^* was integrated to the likelihood-based SECR framework. The likelihood of SECR is a product of the Poisson process likelihood that k individuals were observed at least once and the conditional likelihood of capture history given k individuals, which follows a multinomial distribution (Borchers & Efford, 2008). Activity

centers are latent variables included in both parts, and they were marginalised over spatial domain $\mathcal{S}$. For a simple case that the ln(population density) ρ is constant over space, the likelihood function is

$$L(\boldsymbol{\theta}, \rho) = \frac{\{exp(\rho)a(\boldsymbol{\theta})\}^k exp\big(-exp(\rho)a(\boldsymbol{\theta})\big)}{k!} \times \binom{k}{k_1, k_2, \ldots, k_C} \prod_{i=1}^{k} \frac{\int_{\mathcal{S}} Pr(\omega_i | \boldsymbol{\mu}, \boldsymbol{\theta}) d\boldsymbol{\mu}}{a(\boldsymbol{\theta})}$$

(eqn. 4)

where $\boldsymbol{\theta}$ is a parameter vector affecting the detection process including γ_0 and $\boldsymbol{\beta}$ mentioned above, and k_1, k_2, …, k_C are frequencies of unique capture histories. $a(\boldsymbol{\theta}) = \int_{\mathcal{S}} p_{.}(\boldsymbol{\mu}, \boldsymbol{\theta}) d\boldsymbol{\mu}$, where $p_{.}(\boldsymbol{\mu}, \boldsymbol{\theta})$ is the probability that an individual whose activity center is $\boldsymbol{\mu}$ is detected at least once. $Pr(\boldsymbol{\omega}_i | \boldsymbol{\mu}, \boldsymbol{\theta})$ is the probability of capture history of the *i*th individual given $\boldsymbol{\mu}$. The capture probability is the product of the likelihood of all detectors and occasions, which depends on the detector type. For example, count data from detectors are often described by a Poisson distribution (Distiller et al., 2020; Efford et al., 2013), Poisson(ω_{ij} | exp(g_0)$E_j p^*(x_j, y_j | \boldsymbol{\mu}, \gamma_0, \boldsymbol{\beta})$), where ω_{ij} is the detection number for the *i*th individual at the *j*th detector, g_0 is log catchability, E_j is survey effort, and $p^*(x_j, y_j | \boldsymbol{\mu}, \gamma_0, \boldsymbol{\beta})$ is the probability density of individual location at detector (x_j, y_j). If iterative surveys using binomial detectors are conducted for *T* occasions, the frequency of detection ω_{ij} follows a binomial distribution, Binomial(ω_{ij} | *T*, 1 - exp(-exp(g_0)$p^*(x_j, y_j | \boldsymbol{\mu}, \gamma_0, \boldsymbol{\beta})$)).

Model parameters ρ, g_0, γ_0, and $\boldsymbol{\beta}$ are estimated using a maximum likelihood method. Although conditional likelihood maximisation can be used for parameter estimation in SECR (Borchers & Efford, 2008), full likelihood maximisation was applied because it has the capacity to deal with complex situations in which population density varies across space. Automatic differentiation of likelihood functions (Auger-Méthé et al., 2017) is not currently available for the model because *p** is derived using an iterative sparse linear solver, but a quasi-Newton algorithm, such as the Broyden–Fletcher–Goldfarb–Shanno (BFGS, Nocedal & Wright, 2006) algorithm with numerical differentiation of log likelihoods, works well.

Simulation study

To test the capacity of ADCR to estimate parameters of connectivity and population density correctly, I used a dataset generated via Monte Carlo simulations of animal movement. The landscape is a rectangular grid system of 50 × 50 (hence, the area is 2500), and animal location was described as a discrete coordinate of grid cells. Arrays of count detectors were set to the range, x = [9, 41] and y = [9, 41], with x and y axis spacing of 4 and 81 detectors.

Simulations were iterated 100 times, and true parameter values and landscape structure were randomly determined in each iteration. For each iteration, a heterogeneous landscape was generated using the R package rflsgen (Justeau-Allaire et al., 2022). Random patches were generated in the landscape by rflsgen with parameters shown in Table S1. For covariate values, 0.5 and -0.5 were assigned to patch and non-patch habitats, respectively. True parameter values were sampled from uniform distributions for each iteration. The ranges of true parameters were set as follows: log population density ρ = (-3, -1), log intensity of drift α_0 = (-1, 0) and coefficient of landscape variable β = (-2, 2). g_0 and β_0 were fixed to -3 and 1, respectively. At the beginning of an iteration, the number of individuals in the landscape was determined by a Poisson distribution with expected value of exp(ρ) × 2500 and activity centers were drawn from a discrete uniform distribution.

The animal movement simulation was run for t = 5000 after 100 burn-in steps for randomising initial locations of individuals. For each time step, we calculated the probability vector of individual locations for all cells given the location at the previous step using the advection-diffusion equation with the explicit method (eqn. 5 in Appendix S1), and the location was sampled from a categorical distribution. When there was a detector in a cell in which an individual was located, the number of detection events was simulated by a Poisson distribution with expectation exp(g_0). Then, single-occasion capture-recapture data were obtained by censoring undetected individuals. An example map of simulated movement and observations of an individual is shown in Fig. 1.

I applied ADCR, LCP-SCR, and basic SECR to the simulated dataset to evaluate the accuracy of estimations. For the three estimators, the deviation of estimates from true values was determined and root mean square error (RMSE) and mean bias error (MBE) were calculated. To show how well ADCR and LCP-SCR reproduce home range shapes, the agreement between true (p^*_{true}) and predicted (p^*_{pred}) probability distributions of individual locations was calculated by an overlapping coefficient (Inman & Bradley, 1989):

$$V(\boldsymbol{\mu}) = \iint_{\mathcal{S}} \; min\left(p^*_{pred}(x, y; \boldsymbol{\mu}), p^*_{true}(x, y; \boldsymbol{\mu})\right) dxdy$$

The overlapping coefficient ranges from 0 (no overlap) to 1 (perfect overlap). To evaluate the average performance over locations for activity center $\boldsymbol{\mu}$, I calculated the overlapping coefficients marginalised over $\boldsymbol{\mu}$ within the range of trap array x = [9, 41] and y = [9, 41] for each model and iteration.

To evaluate the robustness of ADCR and LCP-SCR to deviations in the landscape resolution of data from the true state, I considered an additional scenario in which the available landscape variable was restricted to 1/2 resolution. For the 1/2 resolution scenario, grid cells with side length 2 were used for discretizing space in the model estimations, and the landscape variable was averaged for each grid cell. I compared the density and connectivity estimates for the 1/2 resolution scenario with estimates for the baseline scenario.

All models were estimated using maximum likelihood methods using R 4.1.3 (R Core Team, 2022). The movement simulation and log likelihood function of ADCR was written largely in R language, with some subroutines in C++. The source code is available online (https://github.com/kfukasawa37/adcrtest2). The log likelihood values of LCP-SCR were derived based on the R script by Sutherland et al. (2015), with some modifications by Keita Fukasawa to deal with count detectors and the negative effect of landscape on the cost function. The basic SECR was estimated using the R package secr (Efford, 2022).

Results

For all iterations, estimations of ADCR converged successfully. All parameters of ADCR, including the population density and effect of landscape on connectivity, were estimated in an unbiased way. The true and estimated parameters were on the line y = x, on average (Fig. 2). RMSE and MBE of g_0 were 0.0258 and 0.0109, respectively. The true and predicted home ranges overlapped fairly well. The overlapping coefficients marginalised over activity centers were (0.950, 0.9996) over 100 iterations, and the mean was 0.988 (Fig. 3).

As predicted, population densities estimated by LCP-SCR and basic SECR were robust to true connectivity settings in our simulation experiments. RMSEs and bias of log population density estimated by LCP-SCR and basic SECR were very similar to those of ADCR and were not sensitive to the true effect of landscape on connectivity (Table 1). Effects of landscape on the LCP distance estimated by LCP-SCR were linear, on average, but showed a slightly weaker relationship with the true parameters of connectivity (Pearson's r = -0.988, Fig. S1) than that of ADCR (Pearson's r = 0.995, Fig. 2). The overlapping coefficients of home range predicted by LCP-SCR were lower than those for ADCR over the range of true connectivity parameters, and the discrepancy between predicted and true home range was large when the true effect of landscape on connectivity was far from 0 (Fig. 3). LCP-SCR tended to predict a more blurred and isotropic home range shape than the true home range shape (Fig. S2).

ADCR was robust to mismatches in landscape resolution between the data generating process and model estimation. The log population density and effect of landscape in the 1/2 resolution scenario were almost the same as those for the baseline scenario (Fig. 4ac, slopes of principal axes were 0.999 and 1.05, respectively). Although the population density determined by LCP-SCR was also robust to spatial resolution (Fig. 4b, slope of the principal axis was 1.00), the effect of landscape on connectivity was weaker in the 1/2 resolution scenario than in the baseline scenario (Fig. 4d, slope of principal axis was 0.912).

Discussion

Individual movement is an important driver of spatial patterns of populations, and incorporating movement processes in spatial capture-recapture analysis will facilitate studies of the interplay between individual- and population-level ecological processes (Royle et al., 2018; McClintock et al., 2022). The integration of LCP modeling with spatial capture recapture analysis (Royle et al., 2013; Sutherland et al., 2015) was a great methodological advancement for the simultaneous estimation of population density and ecological distance, but accurate estimation of movement parameters exclusively from capture-recapture data is still difficult (Dupont et al., 2022). In this study, I developed a formal framework for a spatial capture-recapture model including mechanistic home range formation with an explicit theoretical link to animal movement models. Through individual-based simulations of animal movement and detection, ADCR accurately estimated the population density and effect of landscape accurately, even when there was a mismatch in spatial resolution between the data generating process and available data. This property provides an advantage over existing estimators, suggesting that ADCR is an effective approach for estimating population density and random walk-based landscape connectivity.

Landscape connectivity is an important determinant of animal space use, including foraging and reproduction, and hence is related to survival and population dynamics. Predicting connectivity is a focus of research in landscape ecology and crucial for conservation planning (Dickson et al., 2019). Although circuit theory is a powerful tool for connectivity modeling in heterogeneous landscapes, it is limited by the lack of a statistical tool for estimating relative conductance values (Zeller et al., 2012). Estimated effects of landscape variables on diffusion coefficients by ADCR can be directly applied to predict relative conductance for calculating resistance distance. ADCR provides an important tool for objective reasoning in landscape connectivity studies. Estimates obtained by ADCR were robust to different spatial resolutions, which is a favourable characteristic of connectivity measures in circuit theory, which shares the same theoretical foundation of random walk descriptions of animal movement (Hanks &

Hooten, 2013).

The effect of a skewed home range on the accuracy of density estimation by SECR has been studied extensively in ecology (Ivan et al., 2013; Royle et al., 2013; Sutherland et al., 2015; Efford, 2019; Theng et al., 2022). The results of this study were consistent with those of recent studies (Efford 2019; Theng et al., 2022) showing that density estimates are generally robust to deviations in assumptions on the distribution of home range shapes. Although some studies (Royle et al., 2013; Sutherland et al., 2015) have reported that density estimates by basic SECR can be biased under the specific spatial patterns of landscape connectivity, our results indicated that the bias in density averaged over a randomly generated landscape was small. Efford (2019) emphasised the importance of sampling design in space, such as the use of a two-dimensional detector array and avoidance of detector array alignment along landscape features, for the correct estimation of density. Obviously, such sampling designs are also favourable for the precise estimation of landscape effects on home range shape by ADCR. Besides the accurate estimation of population density, the integration of animal movement modeling and capture-recapture can improve scale up from individual to population levels (McClintock et al., 2022), and ADCR is useful for such a purpose.

Joint statistical modeling of animal movement trajectories obtained by GPS loggers and spatial capture-recapture data is an important approach for understanding detailed animal movement processes, while ensuring the generality of results (Dupont et al., 2022). Both ADCR and the step selection function are based on biased random walk models (Duchesne et al., 2015), and ADCR can be applied to joint modeling, retaining consistency between the animal movement model and resultant home range. Although the static home range assumption of ADCR has an obvious advantage in the stability of estimates under a severe data deficiency, intercepts of movement speed and site fidelity are aggregated into a single parameter and not identifiable. Joint modeling of the step selection function and ADCR can overcome this limitation by estimating these parameters separately.

The broad application of SECR in ecology can largely be attributed to its flexibility to incorporate heterogeneity in ecological processes underlying spatial capture recapture data, such as environment-dependent abundance and sex-biased detection (Efford, 2022). Future advances in ADCR should focus on similar functionality. In particular, incorporating heterogeneity in home range size (Efford et al., 2016) as well as heterogeneity in connectivity is a major challenge. Although I focused only on heterogeneous connectivity for simplicity, the simultaneous estimation of environmental dependence for both home range size and connectivity can be achieved by incorporating γ_0 varying with the location of the activity center. Also, the generalisation of ADCR for dealing with temporally open populations driven by birth-death processes (Gardner et al., 2010; Efford & Schofield 2022) would be helpful for analysing long-term capture-recapture data. The development of software tools that enable users to benefit from the flexible nature of ADCR is an urgent task for expanding the application of the method.

Similar to step selection analysis linked with advection-diffusion equations (Potts & Schlägel, 2020), an important assumption of ADCR is that sites of animal detection do not show substantial temporal autocorrelation. In general, this assumption would be valid for capture-recapture data in which the number of detections per individual is not large. However, our approach can be biased if the detectability of individuals is quite high and animal steps are highly correlated due to non-uniform turning angles. Modeling correlated movement with a PDE formalism is still a challenging issue (Patlak, 1953; Wang & Potts, 2017), and future research on this topic has the potential to improve home range representation under more realistic situations.

Spatial capture-recapture is a popular method for abundance analyses in ecology and conservation (Iijima, 2020), and large amounts of data have accumulated. Moreover, recent technical advances in individual identification from environmental DNA (Dugal et al., 2022) and machine observations, such as camera traps (Schneider et al., 2022), will expand the

applicability of capture-recapture approaches to broad taxa. Such capture-recapture data have the potential to advance our understanding of the process of animal home range formation. ADCR will be a useful tool for integrated analyses of capture recapture data incorporating individual- and population-level ecological processes.

Acknowledgements

Yutaka Osada provided valuable comments on the earlier version of the statistical model. This study was supported by JSPS KAKENHI Grant Numbers JP13247736, JP19153418, and by the Environment Research and Technology Development Fund (JPMEERF20194005) of the Environmental Restoration and Conservation Agency Provided by the Ministry of Environment of Japan.

Conflict of interest

The author has no conflict of interest to be declared.

Author contributions

KF conceived the ideas, designed methodology, conducted simulation study and wrote the manuscript.

Data availability

No external data were used in this study.

References

Auger-Méthé, M., Albertsen, C. M., Jonsen, I. D., Derocher, A. E., Lidgard, D. C., Studholme, K. R., Bowen, W. D., Crossin, G. T., & Flemming, J. M. (2017). Spatiotemporal modeling of

marine movement data using Template Model Builder (TMB). *Marine Ecology Progress Series*, *565*, 237–249. https://doi.org/10.3354/meps12019

Beyer, H. L., Gurarie, E., Börger, L., Panzacchi, M., Basille, M., Herfindal, I., Van Moorter, B., R. Lele, S., & Matthiopoulos, J. (2016). 'You shall not pass!': Quantifying barrier permeability and proximity avoidance by animals. *Journal of Animal Ecology*, *85*(1), 43–53. https://doi.org/10.1111/1365-2656.12275

Borchers, D. L., & Efford, M. G. (2008). Spatially explicit maximum likelihood methods for capture–recapture studies. *Biometrics*, *64*(2), 377–385. https://doi.org/10.1111/j.1541-0420.2007.00927.x

Dickson, B. G., Albano, C. M., Anantharaman, R., Beier, P., Fargione, J., Graves, T. A., Gray, M. E., Hall, K. R., Lawler, J. J., Leonard, P. B., Littlefield, C. E., McClure, M. L., Novembre, J., Schloss, C. A., Schumaker, N. H., Shah, V. B., & Theobald, D. M. (2019). Circuit theory applications to connectivity science and conservation. *Conservation Biology*, *33*(2), 239–249. https://doi.org/10.1111/cobi.13230

Diniz, M. F., Cushman, S. A., Machado, R. B., & De Marco Júnior, P. (2020). Landscape connectivity modeling from the perspective of animal dispersal. *Landscape Ecology*, *35*(1), 41–58. https://doi.org/10.1007/s10980-019-00935-3

Distiller, G. B., Borchers, D. L., Foster, R. J., & Harmsen, B. J. (2020). Using continuous-time

spatial capture–recapture models to make inference about animal activity patterns. *Ecology and Evolution*, *10*(20), e6822. https://doi.org/10.1002/ece3.6822

Duchesne, T., Fortin, D., & Rivest, L.-P. (2015). Equivalence between step selection functions and biased correlated random walks for statistical inference on animal movement. *PLOS ONE*, *10*(4), e0122947. https://doi.org/10.1371/journal.pone.0122947

Dugal, L., Thomas, L., Jensen, M. R., Sigsgaard, E. E., Simpson, T., Jarman, S., Thomsen, P. F., & Meekan, M. (2022). Individual haplotyping of whale sharks from seawater environmental DNA. *Molecular Ecology Resources*, *22*(1), 56–65. https://doi.org/10.1111/1755-0998.13451

Dunn, J. E., & Gipson, P. S. (1977). Analysis of radio telemetry data in studies of home range. *Biometrics*, *33*(1), 85–101. https://doi.org/10.2307/2529305

Dupont, G., Linden, D. W., & Sutherland, C. (2022). Improved inferences about landscape connectivity from spatial capture–recapture by integration of a movement model. *Ecology*, e03544. https://doi.org/10.1002/ecy.3544

Efford, M. G. (2019). Non-circular home ranges and the estimation of population density. *Ecology*, *100*(2), e02580. https://doi.org/10.1002/ecy.2580

Efford, M. G. (2022). *secr: Spatially explicit capture-recapture models* (R package version 4.5.6). https://CRAN.R-project.org/package=secr

Efford, M. G., Borchers, D. L., & Mowat, G. (2013). Varying effort in capture–recapture studies. *Methods in Ecology and Evolution*, *4*(7), 629–636. https://doi.org/10.1111/2041-210X.12049

Efford, M. G., Dawson, D. K., Jhala, Y. V., & Qureshi, Q. (2016). Density-dependent home-range size revealed by spatially explicit capture–recapture. *Ecography*, *39*(7), 676–688.

Efford, M. G., & Schofield, M. R. (2022). A review of movement models in open population capture–recapture. *Methods in Ecology and Evolution*, *13*(10), 2106–2118. https://doi.org/10.1111/2041-210X.13947

Fuller, A. K., Sutherland, C. S., Royle, J. A., & Hare, M. P. (2016). Estimating population density and connectivity of American mink using spatial capture–recapture. *Ecological Applications*, *26*(4), 1125–1135. https://doi.org/10.1890/15-0315

Gardner, B., Reppucci, J., Lucherini, M., & Royle, J. A. (2010). Spatially explicit inference for open populations: Estimating demographic parameters from camera-trap studies. *Ecology*, *91*(11), 3376–3383. https://doi.org/10.1890/09-0804.1

Goodwin, B. J., & Fahrig, L. (2002). How does landscape structure influence landscape connectivity? *Oikos*, *99*(3), 552–570. https://doi.org/10.1034/j.1600-0706.2002.11824.x

Hanks, E. M., & Hooten, M. B. (2013). Circuit theory and model-based inference for landscape connectivity. *Journal of the American Statistical Association*, *108*(501), 22–33.

https://doi.org/10.1080/01621459.2012.724647

Hanski, I., Kuussaari, M., & Nieminen, M. (1994). Metapopulation structure and migration in the butterfly *Melitaea Cinxia*. *Ecology*, *75*(3), 747–762. https://doi.org/10.2307/1941732

Hirsch, C. (2007). *Numerical Computation of Internal and External Flows: The Fundamentals of Computational Fluid Dynamics*. Elsevier.

Iijima, H. (2020). A review of wildlife abundance estimation models: comparison of models for correct application. *Mammal Study*, *45*(3), 177–188. https://doi.org/10.3106/ms2019-0082

Inman, H. F., & Bradley, E. L. (1989). The overlapping coefficient as a measure of agreement between probability distributions and point estimation of the overlap of two normal densities. *Communications in Statistics - Theory and Methods*, *18*(10), 3851–3874. https://doi.org/10.1080/03610928908830127

Ivan, J. S., White, G. C., & Shenk, T. M. (2013). Using simulation to compare methods for estimating density from capture-recapture data. *Ecology*, *94*(4), 817–826. https://doi.org/10.1890/12-0102.1

Justeau-Allaire, D., Blanchard, G., Ibanez, T., Lorca, X., Vieilledent, G., & Birnbaum, P. (2022). Fragmented landscape generator (flsgen): A neutral landscape generator with control of landscape structure and fragmentation indices. *Methods in Ecology and Evolution*, *13*(7),

1412–1420. https://doi.org/10.1111/2041-210X.13859

Marrotte, R. R., & Bowman, J. (2017). The relationship between least-cost and resistance distance. *PLOS ONE*, *12*(3), e0174212. https://doi.org/10.1371/journal.pone.0174212

McClintock, B. T., Abrahms, B., Chandler, R. B., Conn, P. B., Converse, S. J., Emmet, R. L., Gardner, B., Hostetter, N. J., & Johnson, D. S. (2022). An integrated path for spatial capture–recapture and animal movement modeling. *Ecology*, e03473. https://doi.org/10.1002/ecy.3473

McRae, B. H. (2006). Isolation by resistance. *Evolution*, *60*(8), 1551–1561. https://doi.org/10.1111/j.0014-3820.2006.tb00500.x

McRae, B. H., Dickson, B. G., Keitt, T. H., & Shah, V. B. (2008). Using circuit theory to model connectivity in ecology, evolution, and conservation. *Ecology*, *89*(10), 2712–2724. https://doi.org/10.1890/07-1861.1

Moorcroft, P. R., & Barnett, A. (2008). Mechanistic home range models and resource selection analysis: A reconciliation and unification. *Ecology*, *89*(4), 1112–1119. https://doi.org/10.1890/06-1985.1

Moorcroft, P. R., & Lewis, M. A. (2006). *Mechanistic Home Range Analysis.* Princeton University Press.

Nocedal, J., & Wright, S. (2006). *Numerical Optimization*. Springer Science & Business Media.

Osada, Y., Kuriyama, T., Asada, M., Yokomizo, H., & Miyashita, T. (2019). Estimating range expansion of wildlife in heterogeneous landscapes: A spatially explicit state-space matrix model coupled with an improved numerical integration technique. *Ecology and Evolution*, *9*(1), 318–327. https://doi.org/10.1002/ece3.4739

Ovaskainen, O. (2004). Habitat-specific movement parameters estimated using mark–recapture data and a diffusion model. *Ecology*, *85*(1), 242–257. https://doi.org/10.1890/02-0706

Ovaskainen, O., Rekola, H., Meyke, E., & Arjas, E. (2008). Bayesian methods for analyzing movements in heterogeneous landscapes from mark–recapture data. *Ecology*, *89*(2), 542–554. https://doi.org/10.1890/07-0443.1

Patlak, C. S. (1953). Random walk with persistence and external bias. *The Bulletin of Mathematical Biophysics*, *15*(3), 311–338. https://doi.org/10.1007/BF02476407

Péron, G. (2019). Modified home range kernel density estimators that take environmental interactions into account. *Movement Ecology*, *7*(1), 16. https://doi.org/10.1186/s40462-019-0161-9

Potts, J. R., & Schlägel, U. E. (2020). Parametrizing diffusion-taxis equations from animal movement trajectories using step selection analysis. *Methods in Ecology and Evolution*, *11*(9), 1092–1105. https://doi.org/10.1111/2041-210X.13406

Qi, Y., & Wu, J. (1996). Effects of changing spatial resolution on the results of landscape pattern

analysis using spatial autocorrelation indices. *Landscape Ecology*, *11*(1), 39–49. https://doi.org/10.1007/BF02087112

R Core Team. (2022). *R: A language and environment for statistical computing* (4.1.3). R Foundation for Statistical Computing. https://www.R-project.org/

Royle, J. A., Chandler, R. B., Gazenski, K. D., & Graves, T. A. (2013). Spatial capture–recapture models for jointly estimating population density and landscape connectivity. *Ecology*, *94*(2), 287–294. https://doi.org/10.1890/12-0413.1

Royle, J. A., Fuller, A. K., & Sutherland, C. (2018). Unifying population and landscape ecology with spatial capture–recapture. *Ecography*, *41*(3), 444–456. https://doi.org/10.1111/ecog.03170

Royle, J. A., Karanth, K. U., Gopalaswamy, A. M., & Kumar, N. S. (2009). Bayesian inference in camera trapping studies for a class of spatial capture–recapture models. *Ecology*, *90*(11), 3233–3244. https://doi.org/10.1890/08-1481.1

Schneider, S., Taylor, G. W., & Kremer, S. C. (2022). Similarity learning networks for animal individual re-identification: An ecological perspective. *Mammalian Biology*, *102*(3), 899–914. https://doi.org/10.1007/s42991-021-00215-1

Signer, J., Fieberg, J., & Avgar, T. (2017). Estimating utilization distributions from fitted step-selection functions. *Ecosphere*, *8*(4), e01771. https://doi.org/10.1002/ecs2.1771

Smouse, P. E., Focardi, S., Moorcroft, P. R., Kie, J. G., Forester, J. D., & Morales, J. M. (2010). Stochastic modeling of animal movement. *Philosophical Transactions of the Royal Society B: Biological Sciences*, *365*(1550), 2201–2211. https://doi.org/10.1098/rstb.2010.0078

Sutherland, C., Fuller, A. K., & Royle, J. A. (2015). Modeling non-Euclidean movement and landscape connectivity in highly structured ecological networks. *Methods in Ecology and Evolution*, *6*(2), 169–177. https://doi.org/10.1111/2041-210X.12316

Theng, M., Milleret, C., Bracis, C., Cassey, P., & Delean, S. (2022). Confronting spatial capture–recapture models with realistic animal movement simulations. *Ecology*, e3676. https://doi.org/10.1002/ecy.3676

Thurfjell, H., Ciuti, S., & Boyce, M. S. (2014). Applications of step-selection functions in ecology and conservation. *Movement Ecology*, *2*(1), 4. https://doi.org/10.1186/2051-3933-2-4

Turner, M. G., O'Neill, R. V., Gardner, R. H., & Milne, B. T. (1989). Effects of changing spatial scale on the analysis of landscape pattern. *Landscape Ecology*, *3*(3), 153–162. https://doi.org/10.1007/BF00131534

Wang, Y.-S., & Potts, J. R. (2017). Partial differential equation techniques for analysing animal movement: A comparison of different methods. *Journal of Theoretical Biology*, *416*,

52–67. https://doi.org/10.1016/j.jtbi.2017.01.002

Zeller, K. A., McGarigal, K., & Whiteley, A. R. (2012). Estimating landscape resistance to movement: A review. *Landscape Ecology*, *27*(6), 777–797. https://doi.org/10.1007/s10980-012-9737-0

Figures and tables

Fig. 1 Example of simulated movement and the detection of an individual. The transparent solid line is the movement path. Open rectangles are traps, and blue circles indicate detection counts. The background tile map indicates zones with high (green) and low (pale red) permeability.

Fig. 2 True vs. estimated parameters by ADCR. Dots and error bars indicate maximum likelihood estimates and 95% confidence intervals. The solid black line is y = x.

Fig. 3 Overlap between true and predicted home ranges by ADCR and SCR-LCP.

Fig. 4 Comparison of estimates between baseline and 1/2 resolution scenarios: log population density by (a) ADCR and (b) SCR-LCP, and effect of landscape on connectivity by (c) ADCR and (d) SCR-LCP. Black and grey lines are y=x and the principal axis, respectively.

Table 1 RMSE and MBE of log density for the three estimators for the baseline scenario. The values binned into three classes of the true landscape effect, β, were also shown.

	RMSE			MBE		
	ADCR	LCP-SCR	basic SECR	ADCR	LCP-SCR	basic SECR
Total	0.0788	0.0789	0.0822	-0.00606	0.00123	0.0125
$\beta < -0.5$	0.0752	0.0762	0.0795	-0.0205	-0.0102	-0.00296
$\lvert\beta\rvert <= 0.5$	0.0677	0.0676	0.0730	0.0130	0.0139	0.0333
$\beta > 0.5$	0.0890	0.0883	0.0906	-0.00499	0.00380	0.0133

Supporting information

Appendix S1 Technical details in finite difference method.

Appendix S2 Supplementary figures.

Fig. S1 Relationship between the true effect of landscape on connectivity and estimated effect of landscape on cost by SCR-LCP. Error bars are 95% CIs.

Fig. S2 Example of true and predicted home ranges by ADCR and SCR-LCP. Red x symbols mark the home range center. Black dots are zones with high permeability.

Appendix S3 Supplementary table.

Table S1 Target parameter ranges for the neutral landscape generator, rflsgen. The parameter names were based on Justeau-Allaire et al. (2022). Parameters not shown were set to default values.

Fig. 1 Example of simulated movement and the detection of an individual. The transparent solid line is the movement path. Open rectangles are traps, and blue circles indicate detection counts. The background tile map indicates zones with high (green) and low (pale red) permeability.

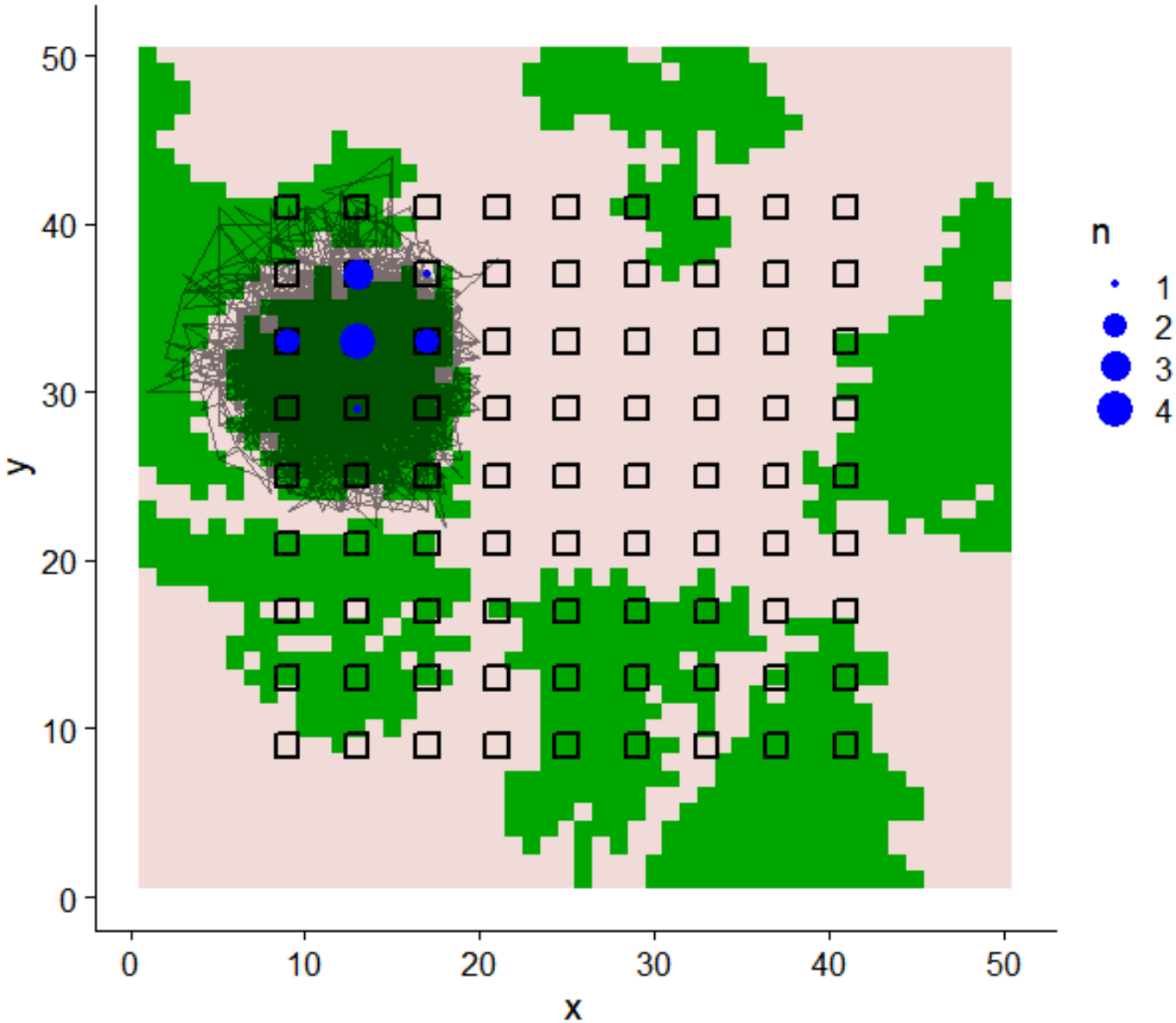

Fig. 2 True vs. estimated parameters by ADCR. Dots and error bars indicate maximum likelihood estimates and 95% confidence intervals. The solid black line is y = x.

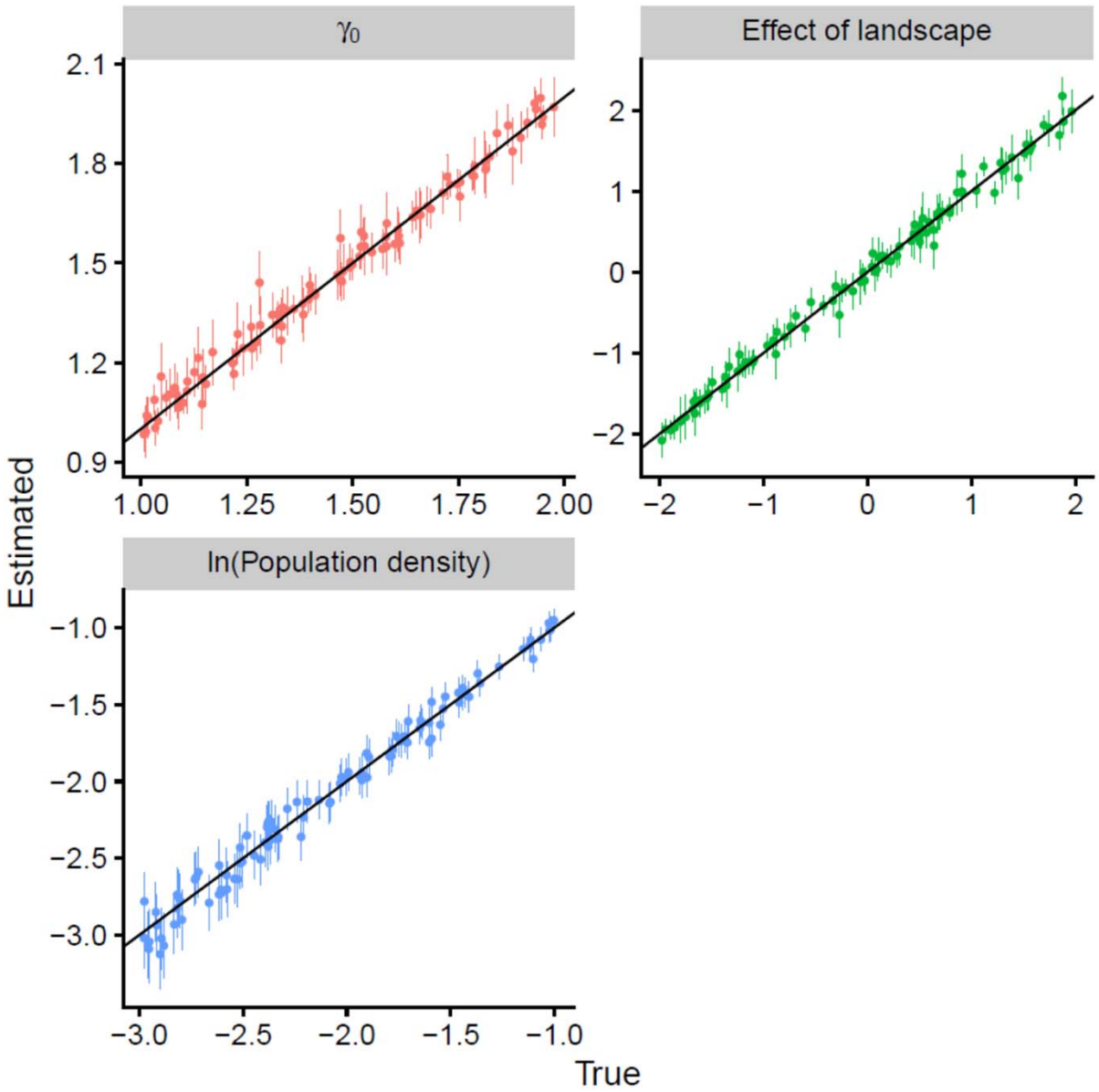

Fig. 3 Overlap between true and predicted home ranges by ADCR and SCR-LCP.

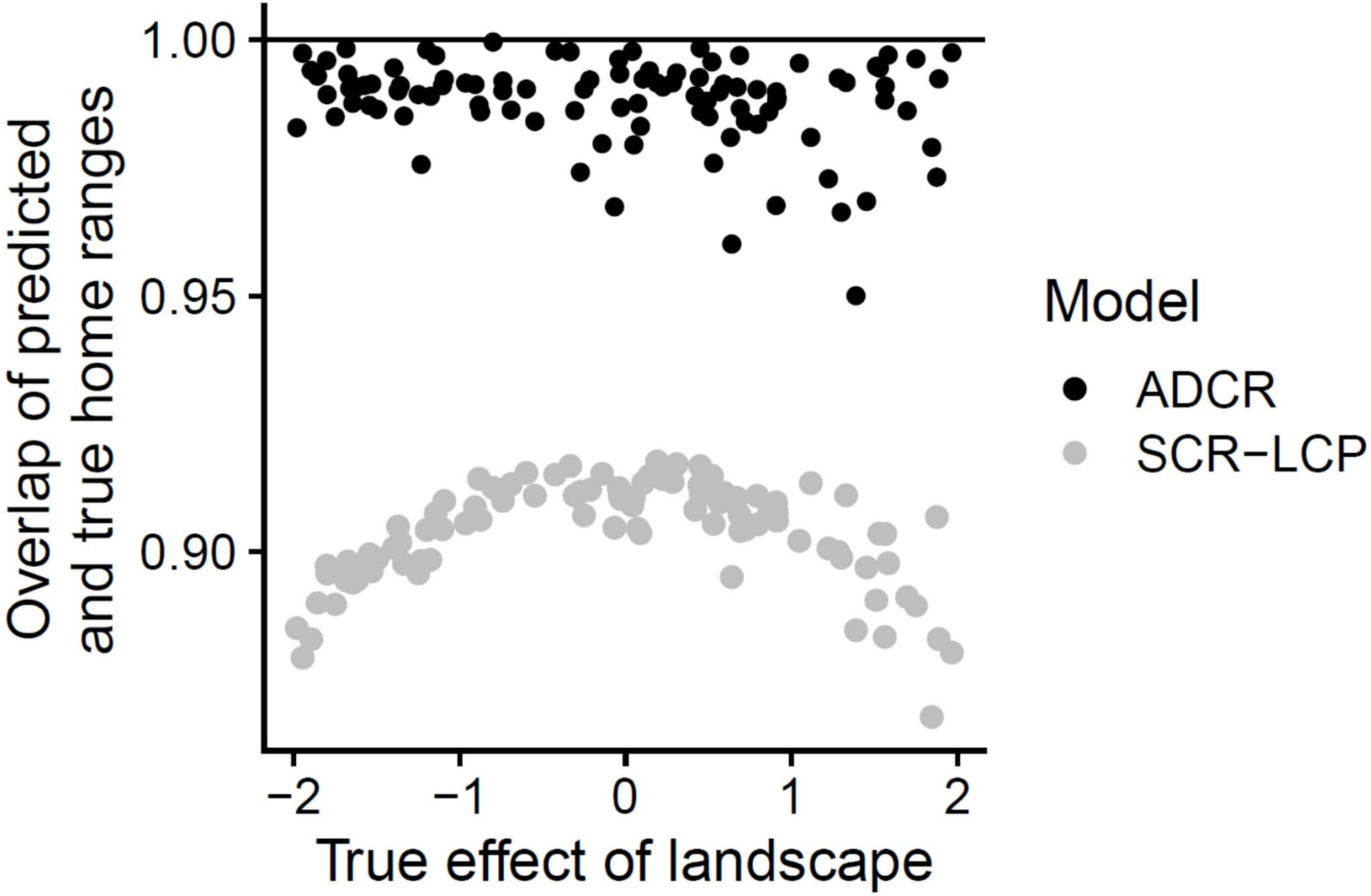
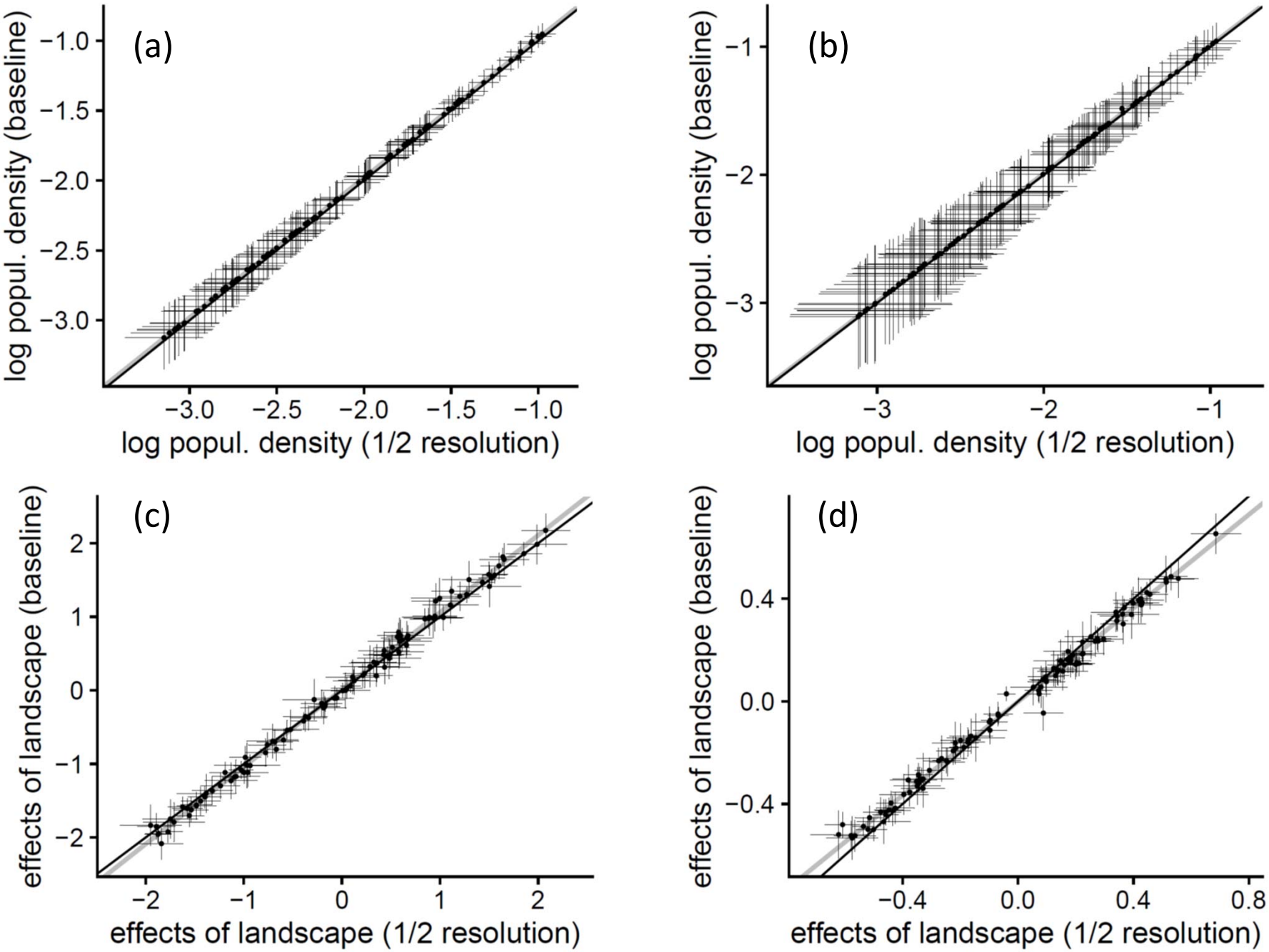
Fig. 4 Comparison of estimates between baseline and 1/2 resolution scenarios: log population density by (a) ADCR and (b) SCR-LCP, and effect of landscape on connectivity by (c) ADCR and (d) SCR-LCP. Black and grey lines are y=x and the principal axis, respectively.